Nigerian Journal of Physics (NJP)
ISSN online: 3027-0936
ISSN print: 1595-0611
DOI: https://doi.org/10.62292/njp.v33i1.2024.181
Volume 33(1), March 2024

Fractional Distribution of Solar UV-B Absorbance on Outdoor Workers within Nsukka Metropolis, South Eastern Nigeria

[1]Sombo, T., *[2]Aka, W. O. and [1]Tyovenda, A. A.

[1]Department of Physics, Joseph Sarwuan Tarka University, Makurdi.
[2]Department of Physics and Astronomy, University of Nigeria, Nsukka.

*Corresponding author's email: williams.aka@unn.edu.ng

ABSTRACT

Ultraviolet radiation is one of the physical concerns of the environment. Several nations have thus moved research attention to this area. This research work aimed at measuring the solar UV-B absorbance on outdoor workers in Nsukka metropolis, South Eastern Nigeria. An LS125 multi probe UV Light Meter with UV- B sensor was used to measure the UV-B irradiance across five study locations representing the various occupations, viz: Barracks (mechanics), Opi (Farmers), Ogige (Traders), Zik's flat (motor park workers) and Onuiyi (Bricklayers). A UV-Vis spectrophotometer was used to determine the change in the optical absorbance of polymer polysulphone dosimeters. Result shows that UV-B Irradiance was highest at solar noon across the study locations. The dosimeter placed on the head received the highest dose of UV- B radiation at the study locations. The values of the cumulative UV-B exposure of the dosimeters placed on the body parts at the study sites were higher than the occupational exposure limit of 30J/m^2 for a 6.5-hour exposure time for both the eye and skin recommended by the International Commission on Non-Ionizing Radiation Protection (ICNIRP). The AIC and BIC values shows that the logarithm regression model outperformed the other models tested. This work therefor sets a reliable baseline data for solar UV-B radiation monitoring in Nsukka, South Eastern Nigeria and also recommend that protective clothing be worn carrying out daily activities during peak solar UV-B radiation hours.

Keywords:
Irradiance,
Absorbance,
Exposure,
Dosimeter
Ultraviolet-B.

INTRODUCTION

Ultraviolet (UV) radiation is electromagnetic radiation with wavelength that falls between the visible and X-ray spectrums. It can be divided into Ultraviolet-A (UV-A, 315–400 nm), Ultraviolet-B (UV-B, 280–315nm) and Ultraviolet-C (UV-C, 100–280nm) based on wavelength (Holick, 2016). As the wavelength gets shorter and more intense, there is a greater chance of harm. UV rays with wavelengths ranging from 290 to 400 nm (nanometers, or billionths of a meter) are exposed to the Earth's surface (Kezic and Zan der Molen, 2023), but humans are protected from this harmful UV rays by the ozone layer that exists above the surface of the earth. Throughout time, however, certain chemicals have been released into the atmosphere, which has damaged the ozone layer. As the ozone layer thins, more UV rays can pass through to the surface of the earth.

Humans can benefit from and suffer harm from sun exposure (Kezic and Van der Molen, 2023). For instance, many processes transform 7-dehydrocholesterol in the skin into vitamin D following UV-B exposure. Vitamin D then influences the body's metabolism of calcium, which is essential for the metabolism of various cell types and bone health (Seckmeyer et al., 2013). Only a small percentage (10%) of the vitamin D in the human body comes from diet; the majority comes from the composite vitamin D irradiated by sunshine (Seckmeyer et al., 2013). Insufficient exposure to sunlight can result in vitamin D deficiency, which can then cause the body to maintain an improper calcium balance, osteoporosis and fragility fractures, and neonatal rickets (Hill and Aspray, 2017).

UV radiation is one of the most important physical concerns in the workplace. As is always the case with agricultural and construction jobs, both governmental and non-governmental organizations anticipate workers to perform their daily tasks during the middle of the day and/or during the dry seasons; this period, the intensity

of the radiation from the sun is always very high (Sombo *et al.,* 2021). Market locations, parking lots, farmlands, playgrounds and job sites in rural areas with little or no ultraviolet protection are where the risk is greatest (Tertsea *et al.,* 2013). Humans are exposed to UV rays in different ways depending on their activities, body posture, personal conduct, and use of UV protection equipment (Sombo *et al.,* 2021).

Since the advent of modern epidemiology, numerous authors have shown a connection between solar UV radiation and cataract, specifically between UV-B radiation and cortical cataract (Löfgren, 2017). Several environmental (Grant, 2016; Estebanez, 2018; Karami *et al.,* 2016; Surdu *et al*., 2013; Mofidi *et al*, 2018) and occupational (Karami *et al*, 2016; Surdu *et al*, 2013; Mofidi *et al*, 2018) epidemiological studies have linked solar exposure to UV radiation with a lower risk of developing different cancers, including colorectal, breast, prostate, kidney, melanoma, and non-Hodgkin lymphoma. A study by Lucas *et al*, (2015) reveals that the majority of sunburns and skin cancers are caused by exposure to UV-B radiation. Because UV-B is efficiently absorbed by DNA, it is believed that UV-B is the primary carcinogen in sunshine (Hart and Norval, 2018). According to a study by Zhu *et al.,* (2015), areas with greater levels of ambient UV-B radiation have higher rates of cataract development. However, UV-A may also be carcinogenic in the skin and can generate reactive species that damage DNA but it is weakly absorbed by DNA (Hart and Norval, 2018). The UV-B spectrum has impacts on antigen presentation inhibition, immunosuppressive cytokine production, and DNA damage, which is a biological trigger for UV-mediated immunosuppression (Katiyar *et al*, 2017).

According to Lucas e*t al.,* 2015 numerous studies have looked at solar UV-B exposure and its effects on skin for persons who work outside or engage in sun-related activities. However, based on literature, no information is available on measurement and modeling of Solar UV-B absorbance in Nsukka metropolis. The aim of this study is to measure and model the Solar UV-B absorbance on outdoor workers (farmers, bricklayers, mechanics, transport workers and traders) in Nsukka, Enugu State. It will measure the UV-B Irradiance and calculate the UV-B index in the different study locations.

MATERIALS AND METHODS

Study Location

Nsukka, a Local Government Area in Enugu State is located at latitude 6°50'N – 6°58'N and longitude 7°22'E – 7°31'E with ground elevation of 439.3m above sea level. The local government headquarters is sited at the hilly and green areas that Nsukka is known for. The vegetation of Nsukka plateau is divided into five sub-types: (i) Grasslands, (ii) Farmlands on derived savanna, (iii) Mosaic farmland/oil palm forests, (iv) Wooded shrub grasslands/woodland and (v) Mature nature forests. In 2006, Nsukka had a population of 309,633 comprising mainly of people who engage in civil service duties, commercial activities and agrarian peasantry. The prestigious first indigenous University of Nigeria is located at Nsukka and was founded in 1960 by late Dr. Nnamdi Azikiwe, first President of Nigeria.

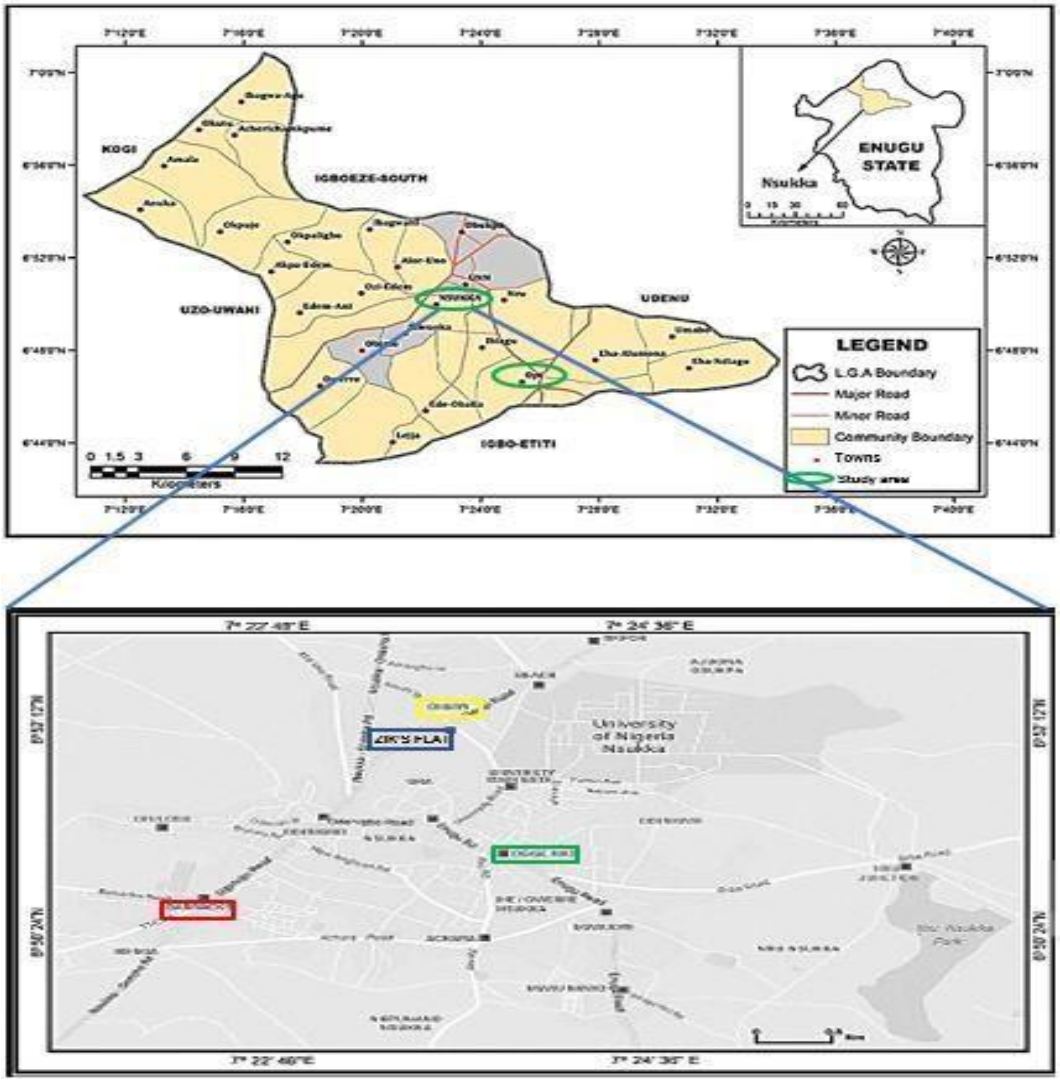

Plate 1: Map of Nsukka Local government Area indicating selected Study Sites

Materials used

The following materials were used in this researc

1. An LS125 multi probe UV light Meter with UV-B Sensor
2. Twelve-channel GPS
3. Polymer polysulphone dosimeters (2cm by 2cm)
4. UV/Vis spectrophotometer.

Plate 2: UV/Vis Spectrophotometer Serial No. 756S, Designed by Hinotec Lab Equipment, Ningbo, China

Plate 3: An LS125 Multi Probe UV Light Meter

Procedure

1. An LS125 multi probe UV Light Meter designed by Linshang Technology Co. Ltd, China was used to measure the UV-B irradiance across the study locations.
2. A twelve-channel *etrex* GPS designed by Garmin Ltd, USA was used to take measurement of the longitude, latitude and altitude of the measurement sites.
3. Some pieces of 2cm X 2cm polymer polysulfone dosimeter from Parisi, Queensland University were used in this work. Some were placed on different parts of a human manikin at different locations representing the occupations viz: Barracks (mechanics), Opi (farmers) and Ogige market (traders); while some were used for calibration. The research was carried out during the month of May/June 2023.
4. A UV/Vis spectrophotometer serial no. 756S, designed by Hinotec Lab equipment, Ningbo, China was used to take the pre and post absorbance measurement of the polysulphone dosimeters at the Nano technology Lab. of the University of Nigeria, Nsukka. The optical absorbance was then calculated as the difference between the pre absorbance and the post absorbance measurement.

Dosimeter calibration

At the measuring site, the dosimeters were calibrated. This was accomplished by exposing five dosimeters at

each of the three locations on a horizontal plane to enable the dosimeters quantify UV-B exposures in J/m^2. The desired quantity was calculated using equation 1 below:

Exposure quantity (J/m^2) – Calibration factor (Constant) x Absorbance (1)

The calibration factor is often taken as the gradient of the calibration curve.

Prediction of UV-B irradiance using Newton divided difference

In order to have an idea about the UV-B irradiance of outdoor workers in between the hours which data was collected, predicting formulas were obtained using Newton Divided

Interpolation. Given a function:

$y = f(x)$ (2)

which may be a set of data points between y_n and x_n.

The process of finding the value of y corresponding to any value of $x = x_i$ between x_0 and x_n is referred to as interpolation. Thus, Interpolation is the technique of estimating the value of a function for any intermediate value of the independent variable.

In this study, Newton Divided difference interpolation was used to construct predicting functions using the data collected from the field at different locations.

To construct Newton Divided Difference Interpolating polynomials, let the nodes or arguments be defined by $x_k = x_0, x_1, x_2,\ldots,x_n$ and the unknown function $f(x_k)$. The coefficients of Newton divided difference polynomial are obtained from Table 4.

Once the coefficients are obtained for Table 5 for each k = 0, 1, 2… n, Newton Divided

Difference Polynomial is given by equation 5;

$(x) = f[x_0] + \sum_{k=1}^{n} f[x_0\, x_1, \ldots, x_k](x - x_0) \ldots (x - x_{k-1})$ (3)

Equation (5) was applied to get the required predicting function at the various study sites. The generated equation was thereafter plotted into Mat lab to obtain accurate values.

Method of applying mathematical models to analyze UV-B absorbance

Linear, polynomial and logarithm regression model was applied to UV-B absorbance in the study location. The models were tested using the Akaike information criterion (AIC) and the Bayesian Information Criterion (BIC).

The AIC is given by:

AIC = 2K - 2ln (L) (4)

K is the number of independent variables used and L is the log-likelihood estimate (a.k.a. the likelihood that the model could have produced your observed y-values). The default K is always 2, so if your model uses one independent variable your K will be 3, if it uses two independent variables your K will be 4, and so on.

The formula for BIC is:

BIC = ln (n)k – 2ln (L) (5)

Calculation of UV-B index

The UV-B Index was calculated using the relation as stated in equation below:

$I_{uv} = \frac{E_{ery}}{25}$ (6)

Where E_{ery} is erythemally effective UV-B Irradiance..

RESULTS AND DISCUSSION

Results

Table 1 presents the result of the UV-B Irradiance at the various study sites and predicted irradiance values (written in blue). Tables 2, 5 and 8 respectively shows result of the cumulative UV-B exposure of dosimeters at Barracks, Opi and Ogige market respectively. Additionally, Figures 1, 5 and 9 presents result of dosimeter calibration at the study sites while Figures 2, 6 and 10 presents the result of the dosimeter response curve at the locations considered. The result of the UV-B absorbance of the polysulphone placed on various parts of the manikin for three study locations considered are presented in Figures 3, 7 and 11. Figure 4, 8 and 12 prsents the result of the linear, polynomial and logarithm fit of the relationship between UVB absorbance and irradiance at the various study sites while Figure 13 presents the ranges of value for UV-B absorbance and cumulative exposure. Additionally, Figure 14 shows result of the cumulative UV-B exposure on the different body parts at Barracks, Opi and Ogige. Figure 15 presents the result of the calculated UV-B index in the entire study.

Table 1: UVB Irradiance at the Study Sites and Predicted Irradiance in-between Experimental Hours

S/N	Sites	Hourly Measurements (W/m^2)					
		10am	11am	12pm	1pm	2pm	3pm
1	Opi	1.949	2.220	2.478	2.662	1.948	1.780
2	Ogige	1.871	1.994	2.460	2.614	1.951	1.699
3	Barracks	2.077	2.471	2.661	2.812	2.493	2.100
4	Onuiyi	1.661	1.782	1.812	1.997	1.800	1.628
5	Zik's flat	1.684	1.793	1.801	2.340	1.947	1.561

Table 2: Cumulative UV-B Exposure at Barracks

Tag No	Dosimeter Exposure Time(min)	UVB Irradiance for exposure (W/m^2)	Post Abs. of polysupl-sulphone	Change In optical Abs Abs. (ΔA_{330})	Approx UV-B exposure (J/m^2)	Cumm UVB exposure (J/m^2)
1	30	2.077	0.311	0.200	62.310	62.310
2	60	2.472	0.401	0.283	148.320	210.630
3	90	2.661	0.443	0.340	239.490	450.120
4	120	2.813	0.583	0.478	337.560	787.680
5	150	2.493	0.620	0.508	379.950	1167.630

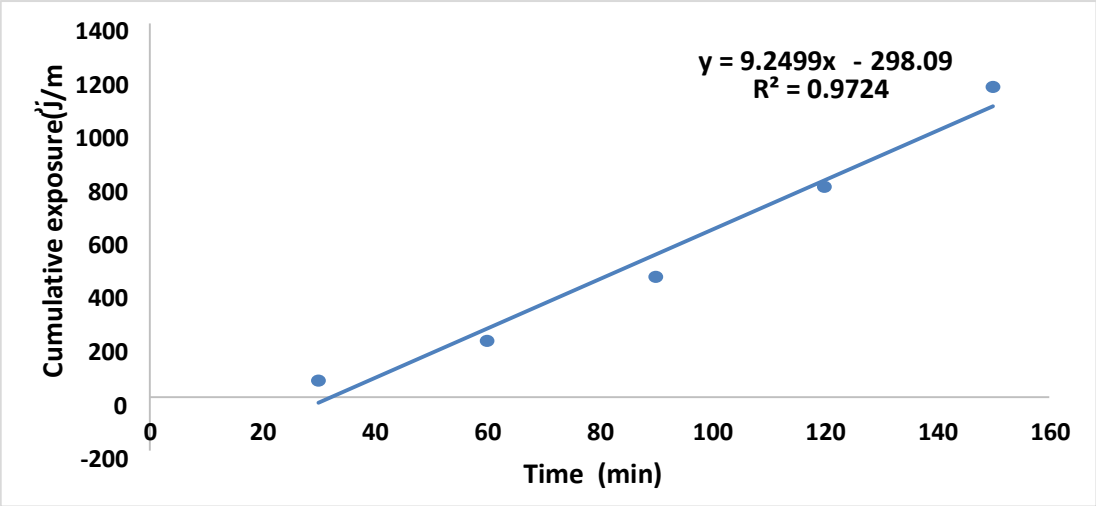

Figure 1: Dosimeter Calibration Curve at Barracks

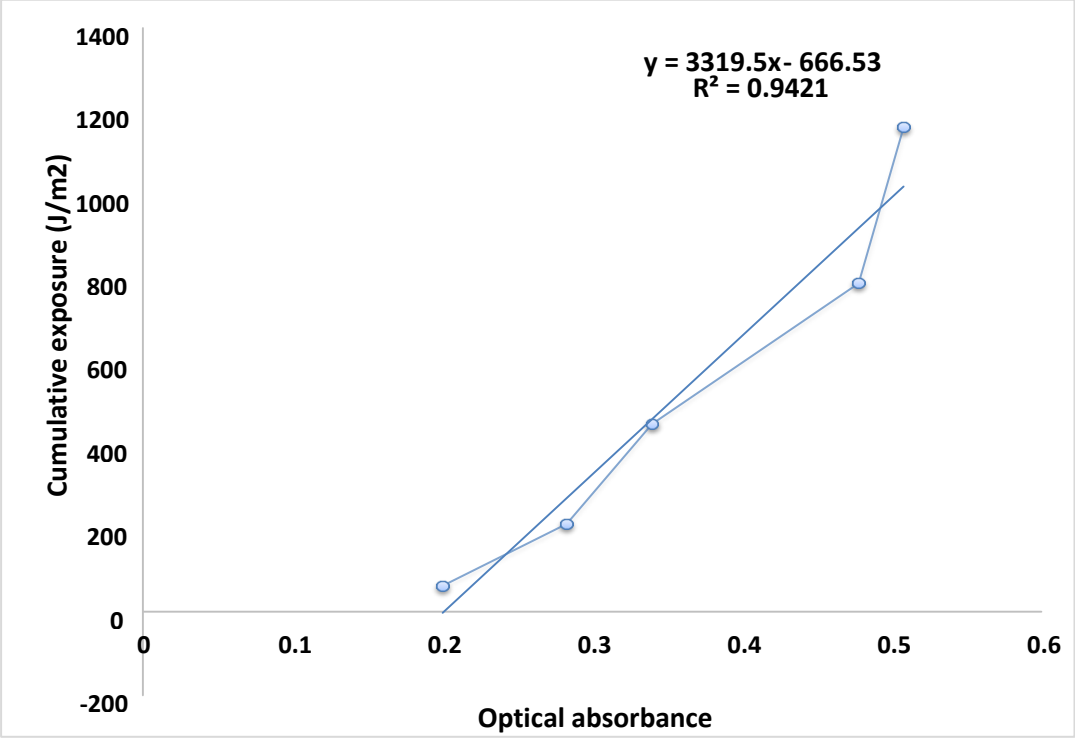

Figure 2: Polymer Polysulphone Dosimeter Response Curve at Barracks

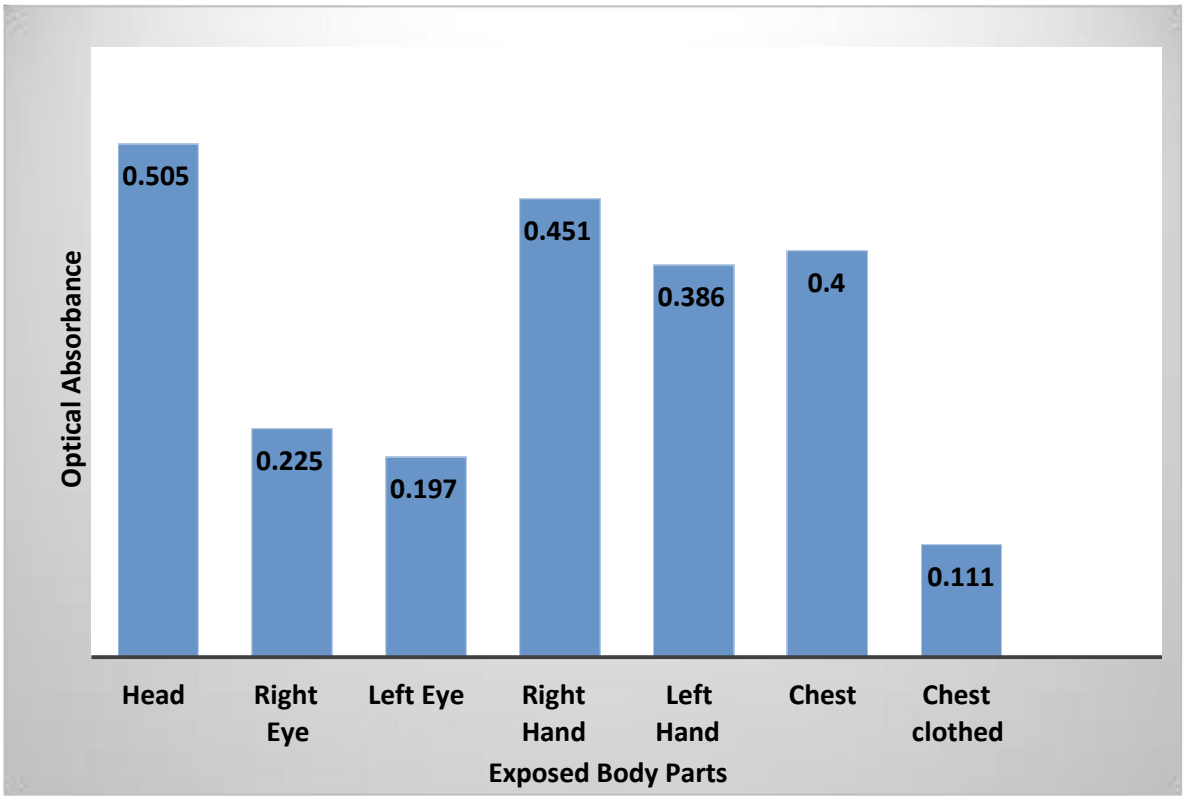

Figure 3: UV-B Optical Absorbance on different Body Parts at Barracks

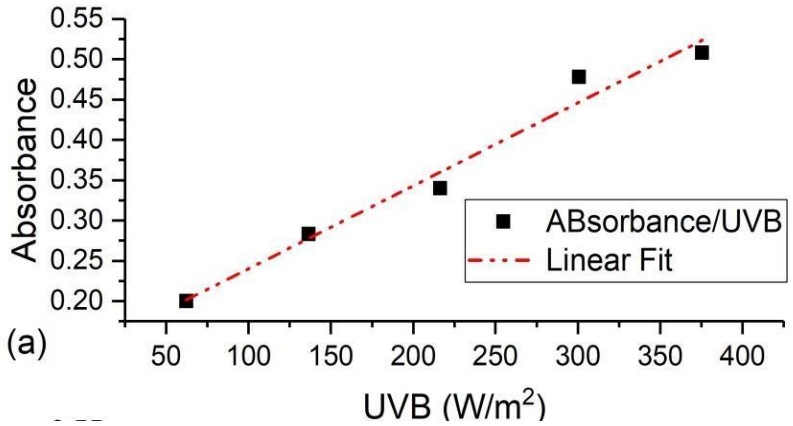

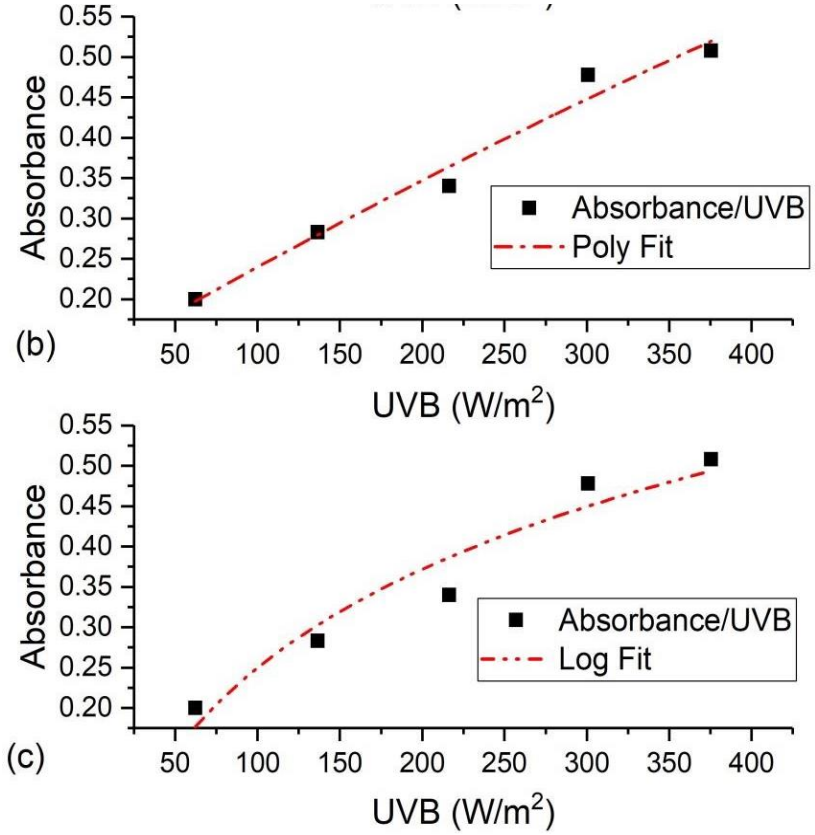

Figure 4: (a) Linear, (b) polynomial and (c) Logarithm fit for the Relationship between Absorbance and UV-B Irradiance at Barracks

Table 3: Summary of Model Constants at Barracks

	Model	Equation	R-square
	Linear	$y = 0.001x + 0.1374$	0.975
	Polynomial	$y = -3E\text{-}07x^2 + 0.0012x + 0.1257$	0.976
Barracks	**Logarithm**	$y = -0.803 + 0.216 \exp(31x)$	0.879

Table 4: Summary of AIC and BIC for Barracks

	Model	AIC	BIC
	Linear	-19.59	-26.07
	Polynomial	-18.07	-19.63
Barracks	**Logarithm**	-7.11	-8.29

Table 5: Cumulative UV-B Exposure at Opi

Tag No	Dosimeter Exposure Time(min)	UVB Irradiance for exposure (W/m^2)	Post Abs. of polysupl-sulphone	Change In optical Abs Abs. (ΔA_{330})	Approx UV-B exposure for each (J/m^2)	Cumm UVB exposure (J/m^2)
27	20	1.949	0.311	0.205	38.980	38.980
28	40	2.323	0.341	0.231	92.920	131.900
29	60	2.478	0.499	0.383	148.680	280.580
30	80	2.664	0.561	0.442	213.120	493.700
31	100	1.948	0.593	0.491	194.800	688.500

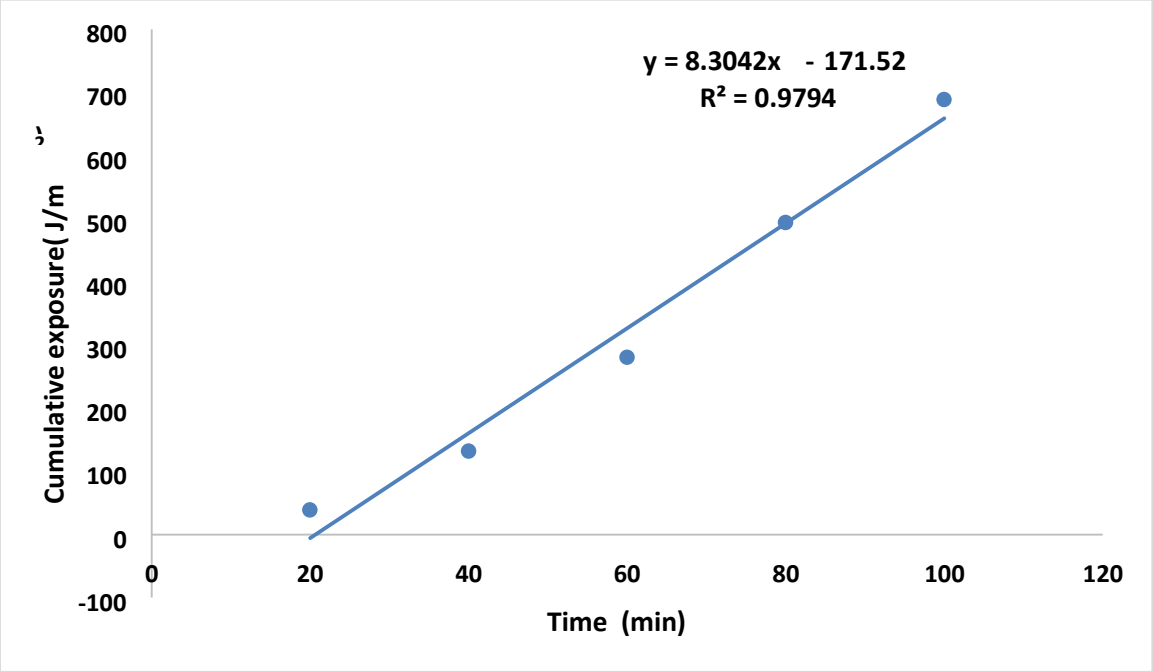

Figure 5: Dosimeter Calibration Curve at Opi

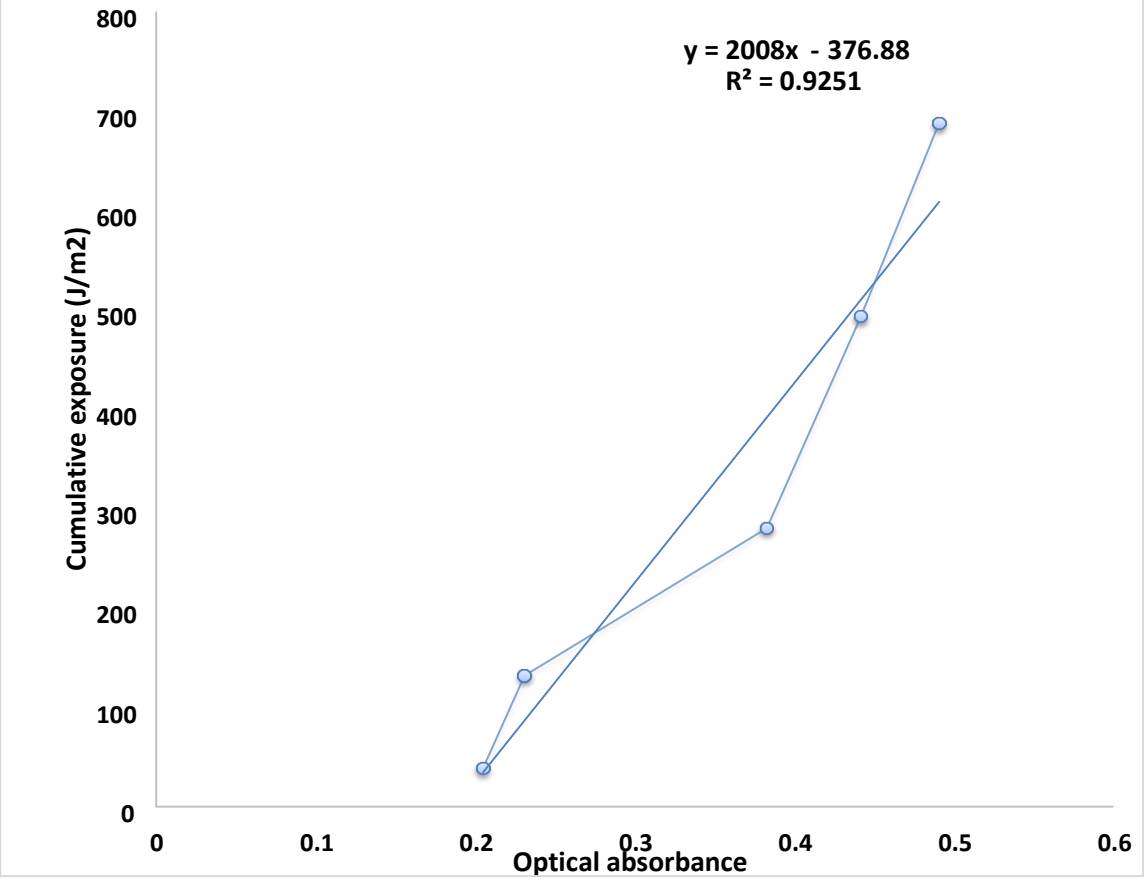

Figure 6: Polymer Polysulphone Dosimeter Response Curve at Opi

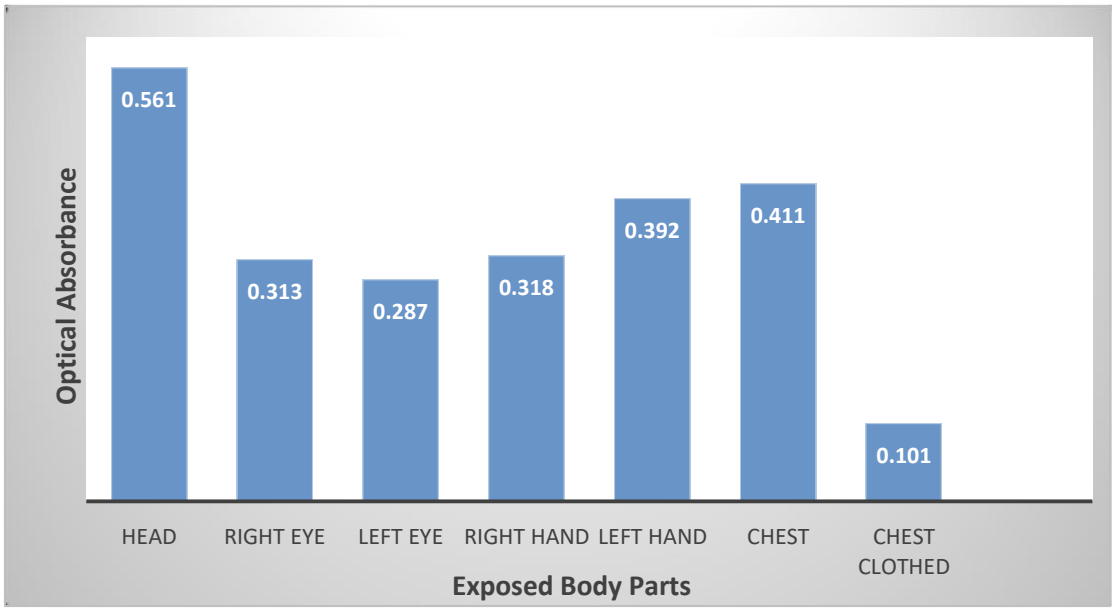

Figure 7: UV-B Optical Absorbance at Opi

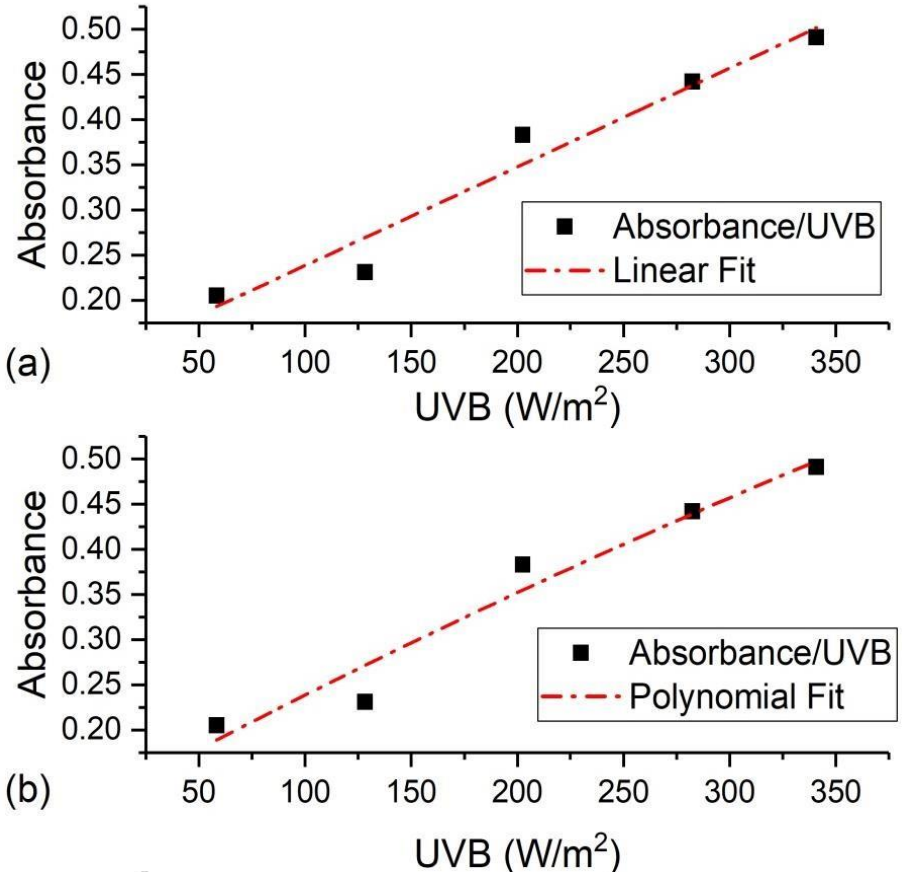

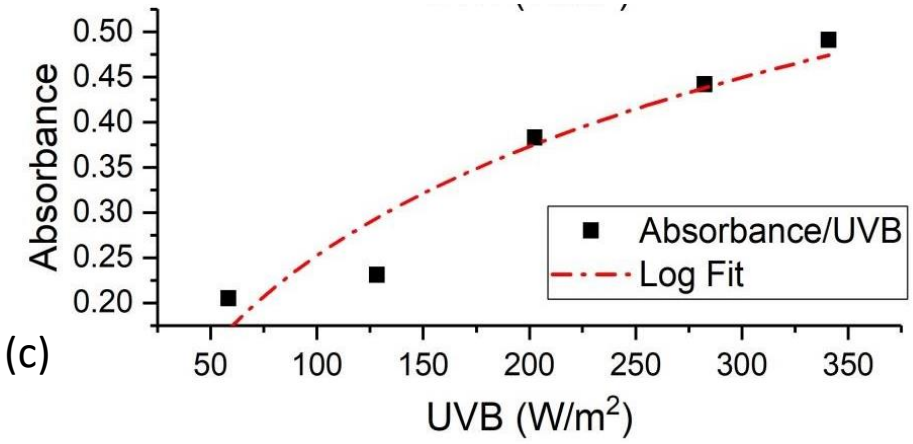

Figure 8: (a) Linear, (b) Polynomial and (c) Logarithm fit for the Relationship between Absorbance and UV-B Irradiance at Opi Farm

Table 6: Summary of Model Constants for Opi

	Linear	y = 0.0011x + 0.1292	0.9568
	Polynomial	y = -4E-07x^2 + 0.0013x + 0.1167	0.9577
Opi	**Logarithm**	y=-0.773+0.211exp(29x)	0.915

Table 7: Summary of AIC and BIC for Opi among Farmers

	Model	**AIC**	**BIC**
	Linear	-17.26	-18.43
	Polynomial	-15.37	-16.92
OPI	**Logarithm**	-4.11	-5.28

Table 8: Cumulative UV-B exposure at Ogige Market

Tag No	**Dosimeter Exposure Time (min)**	**UVB Irradiance for exposure (W/m^2)**	**Post Abs. of polysupl-sulphone**	**Change In optical Abs Abs. (ΔA_{330})**	**Approx UV-B Exp for each interval (J/m^2)**	**Cumm UVB exposure (J/m^2)**
14	10	1.873	0.238	0.121	18.730	18.730
15	20	1.994	0.310	0.199	39.380	58.610
16	30	2.463	0.359	0.244	73.890	132.50
17	40	2.614	0.398	0.295	104.560	237.060
18	50	1.951	0.449	0.342	97.550	334.610

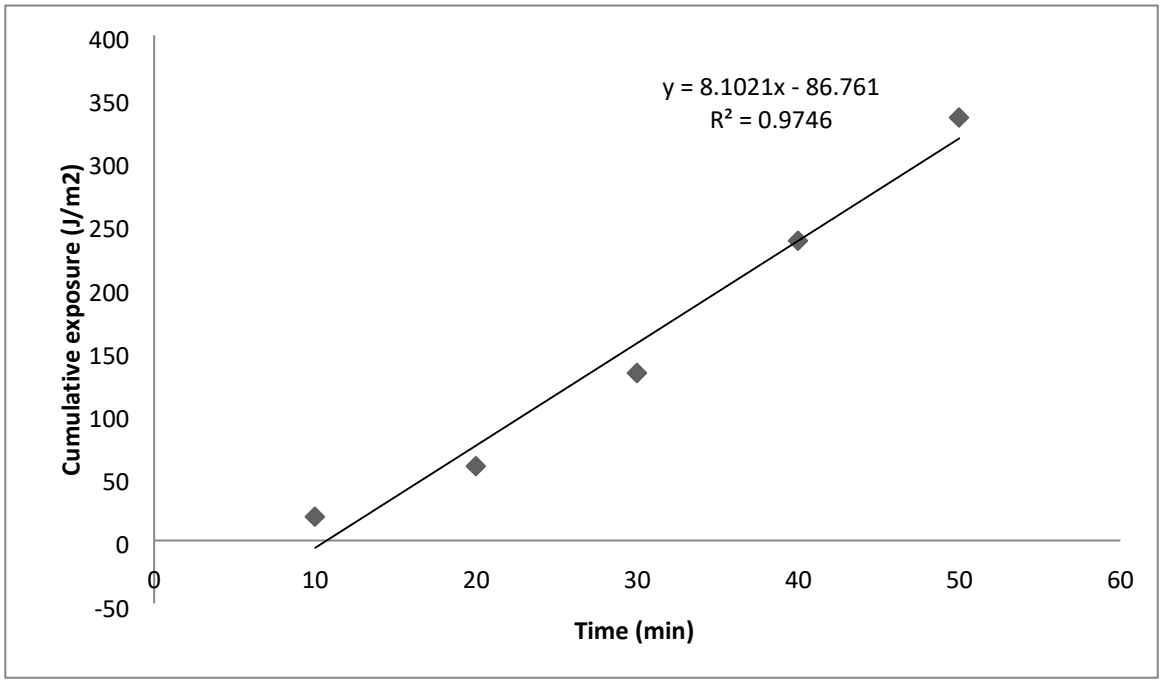

Figure 9: Dosimeter Calibration Curve at Ogige

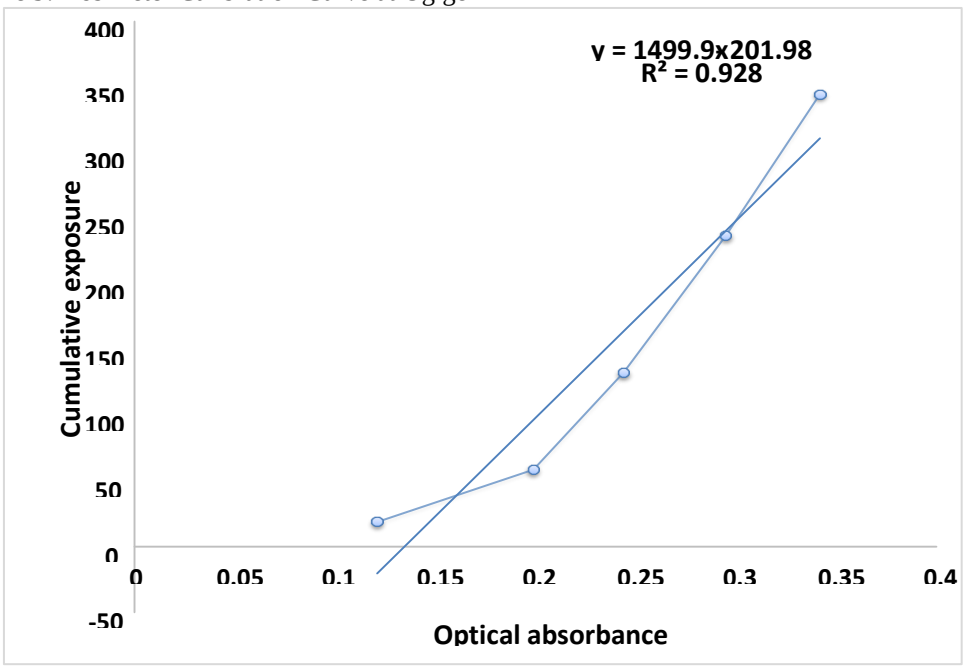

Figure 10: Polymer Polysulphone Dosimeter Response Curve at Ogige Market

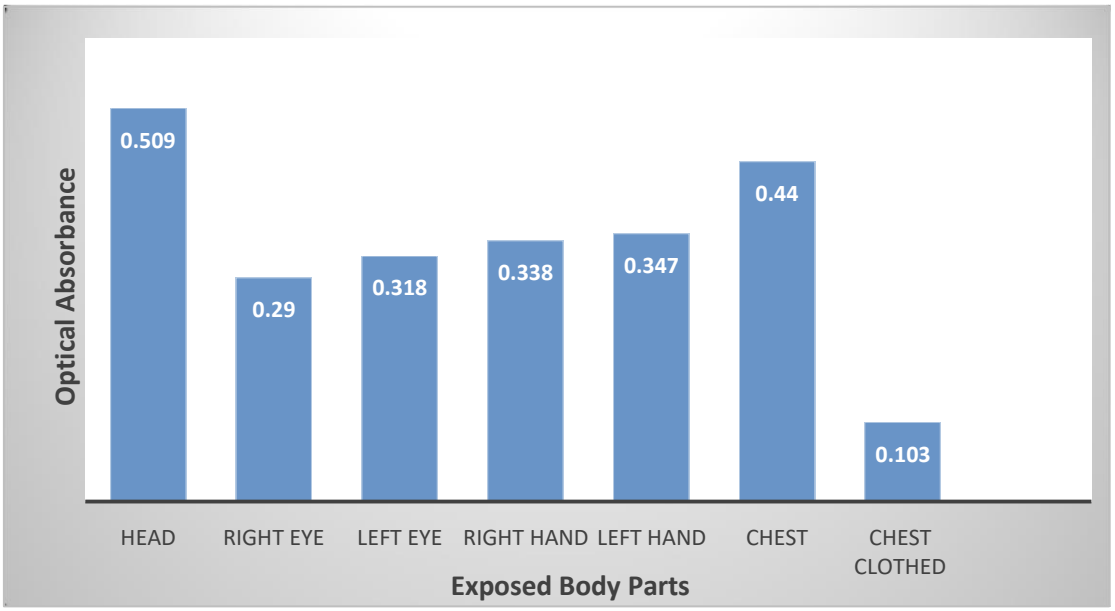

Figure 11: UV-B Absorbance against Exposed Body Parts at Ogige

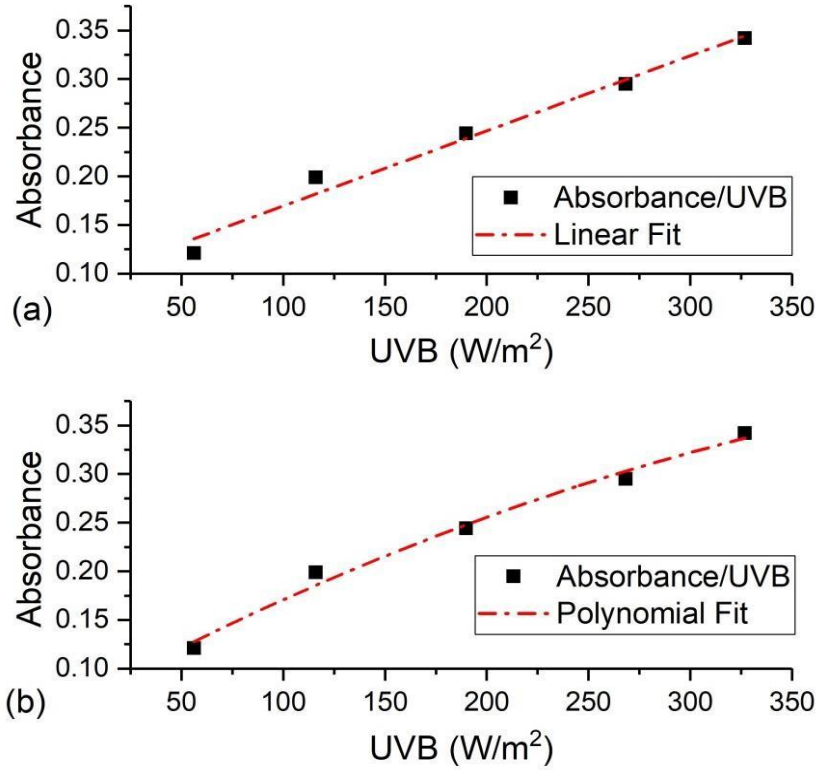

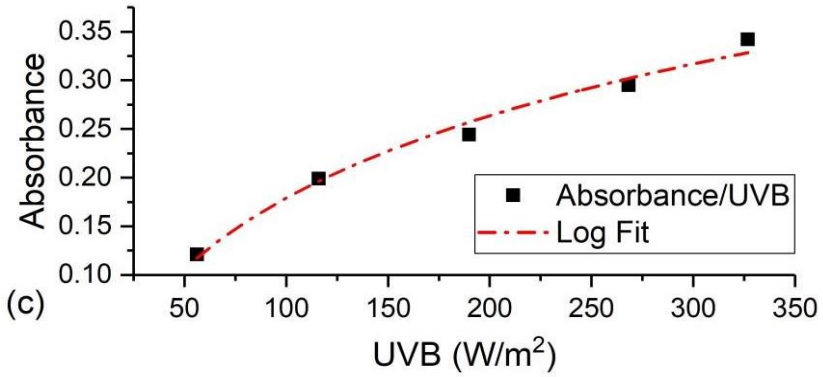

Figure 12: (a) Linear, (b) polynomial and (c) Logarithm fit for the relationship between Absorbance and UV-B Irradiance at Ogige Market

Table 9: Summary of Model Constants for Ogige Market

	Linear	y = 0.0008x + 0.0924	0.9808
	Polynomial	$y = -9E-07x^2 + 0.0011x + 0.0676$	0.9886
Ogige Market	**Logarithm**	y=-0.532+0.147exp(28x)	0.9783

Table 10: Summary of AIC and BIC for Ogige market

	Model	**AIC**	**BIC**
	Linear	-25.27	-26.45
	Polynomial	-25.90	-27.46
Ogige	**Logarithm**	-2.65	-3.82

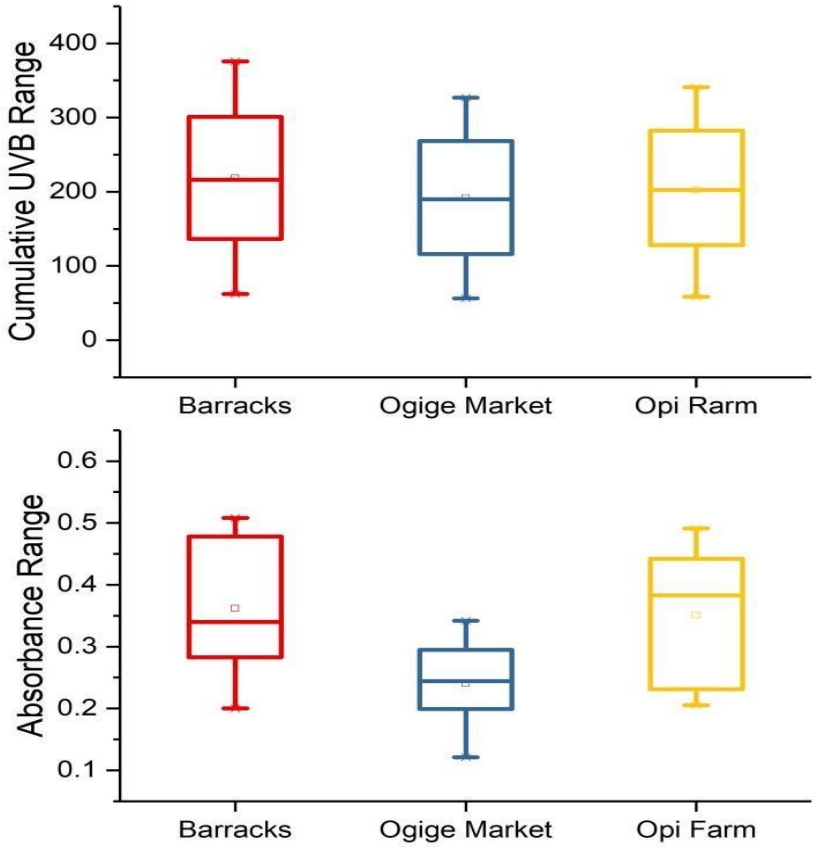

Figure 13: Ranges of values for UV-B Absorbance and Cumulative UV-B Exposure

Cumulative UV-B Exposure of Dosimeters placed on various Body Parts among the various Occupations

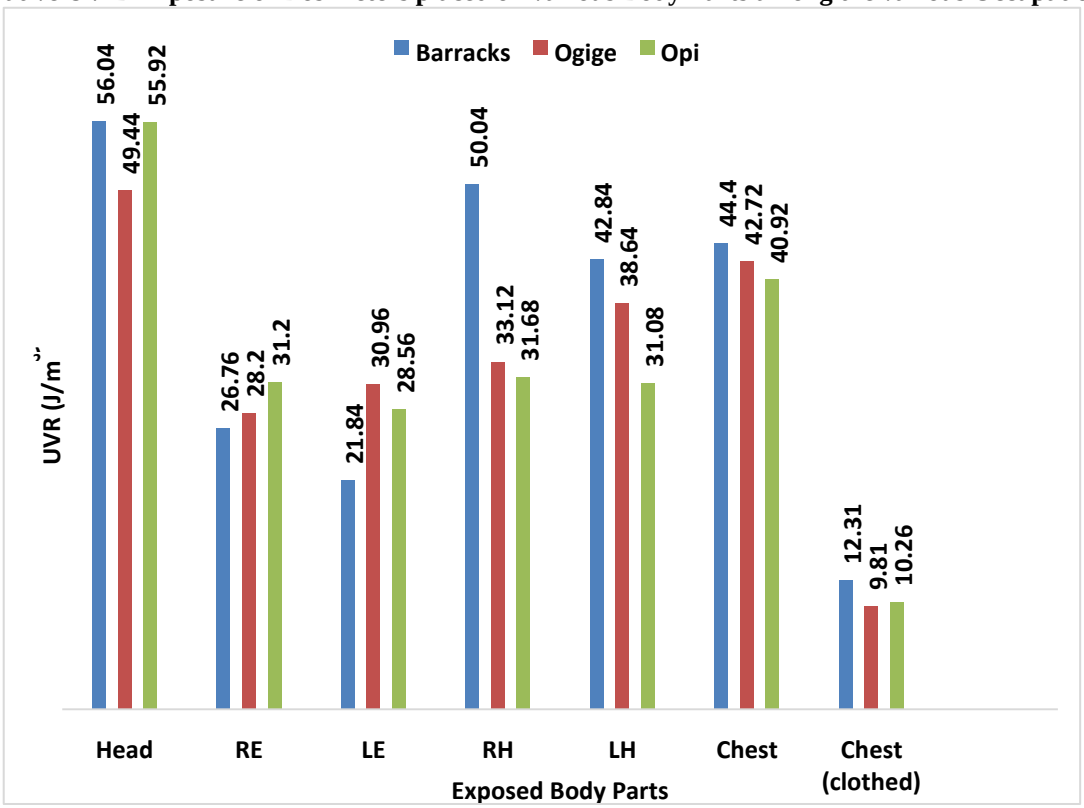

Figure 14: Exposure Quantity of Dosimeters placed on various Body Parts

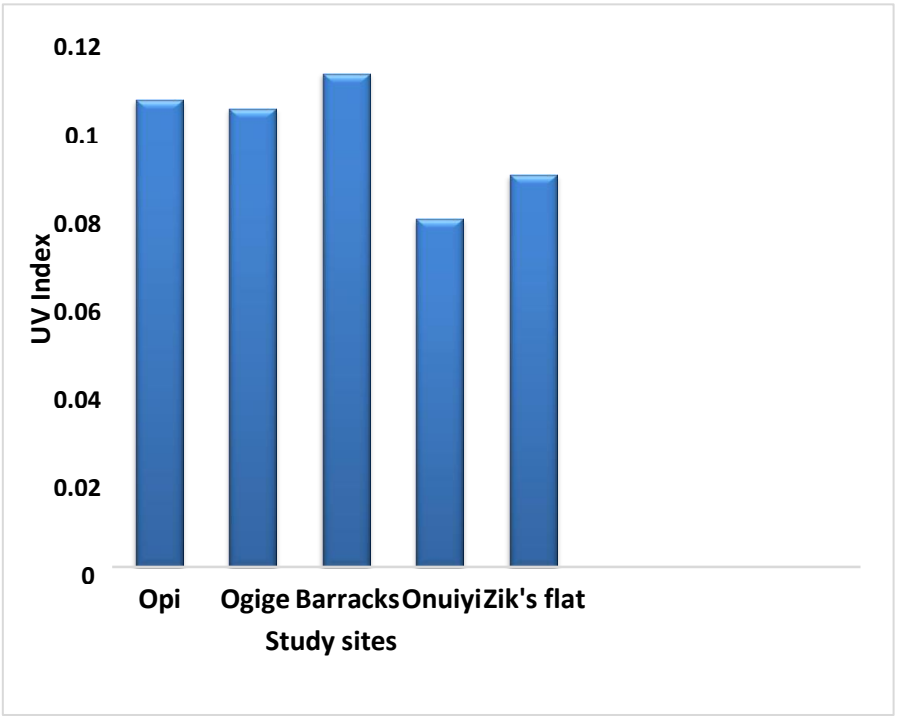

Figure 15: UV-B Index at the various study sites

Discussion

The result of the UV-B irradiance values (Table 1) measured at different hours of the day and at the different study sites, and the predicted values in between experimental hours (written in blue) shows that solar UV-B irradiance was highest between the hours of 12pm and 2pm with the highest value 2.66 W/m^2 by 12 pm at Barracks. The lowest value was recorded by 3pm at Onuiyi. The irradiance is typically strongest between the hours of 12pm and 2pm due to high sun intensity present during this time within the area. The values of irradiance for hours in between measurement periods were predicted using Newton Divided Difference. From the predicted data, the results show high level of accuracy as the difference between the data points and predicted values were in the error range of 0.001to 0.39.

The dosimeters recorded high cumulative exposure of 1167.630J/m^2, 688.5J/m^2 and 334.6J/m^2 for Barracks, Opi and Ogige study sites respectively. These values are higher than the occupational exposure limit of 30J/m^2 for a 6.5-hour exposure time for both the eye and skin recommended by the International Commission on Non-Ionizing Radiation Protection (ICNIRP) and it goes in line with the results obtained by Sombo *et al.,* (2021) who measured the occupational exposure to solar UV radiation in Makurdi metropolis, Benue state, central Nigeria using a digital UV broadband meter. From their findings, the cumulative exposure estimated for traders in north bank car park was 610.98J/m^2. According to the study, these values are quite high and they recommended that risky behaviors which would lead to both acute and chronic effects should be minimized.

The dosimeter response curve for cumulative UV-B exposure versus absorbance at the three study sites under consideration shows an almost linear line which indicates a strong relationship between increasing exposure to UV-B radiation and absorbance in the measured interval of the calibration time during peak solar noon; this period was chosen amid zero cloud cover due of high intensities of solar radiation usually experienced around this time. From the result of the UV-B absorbance on different body parts across the different occupations, the head part recorded the highest UV-B absorbance at the three study locations. This could be as a result of the head facing direct radiation from the sun. However, the eye recorded the lowest UV-B absorbance across the locations. However, under cloth cover, the dosimeter on the chest recorded a very low value at the study locations. This result goes in line with that of Tersea *et al.,* 2013 who measured the average solar UV-B radiation dosimetry in central Nigeria using a digital UV broadband meter, the Educator (N0. P3-6510), obtained from Ann Arbor, U.S.A. From their result, the dosimeter placed on the head had the highest optical absorbance of 0.65 while dosimeter placed on the right eye had the lowest optical absorbance 0.24. The result also shows that the clothing we put on also helps to shield us from UV-B radiation.

The results presented in Figure 13 illustrate the ranges of cumulative UV-B (independent variable) and absorbance (dependent variable) across the study sites. Barracks exhibited the highest cumulative UV-B and absorbance, followed by Opi Farm and then Ogige Market.

The coefficients for the model fit viz: Linear, Polynomial, and Logarithmic fit aimed to establish the relationship between cumulative UV-B exposure and absorbance response. From the results, the logarithmic model outperformed the other models across all study sites, with AIC values of 7.11, -2.65, and -4.11 for Barracks, Ogige, and Opi Farm, respectively. Similarly, the BIC values for Barracks, Ogige, and Opi were -8.29, -3.82, and -5.28, respectively. Thus, the logarithmic model provides the best fit for the relationship between cumulative UV-B exposure and absorbance response in the investigated locations.

The result of the cumulative UV-B exposure of dosimeters placed on various body parts shows that Barracks, Ogige and Opi recorded the highest cumulative exposure of 56.04J/m2, 49.44J/m2 and 55.92J/m2 respectively. The dosimeter placed on the chest under cloth cover recorded the lowest cumulative UV-B exposure of 12.31J/m2, 9.81J/m2 and 10.26J/m2 at Barracks, Ogige and Opi respectively. The result shows that the clothing we put on helps to shield us from the harmful effects of UV-B radiation. The variation in the values could be as a result of the difference in exposure geometry of the outdoor workers under consideration.

From the results of the calculated UV index, Barracks had the highest value of 0.112, followed by Opi (0.106), Ogige (0.104), Zik's flat (0.089) and Onuiyi (0.079) in that order. These values are however not extreme when compared to the UV index risk ratings by the world health organization (WHO, 2001).

CONCLUSION

The UV-B exposure and cumulative exposure in this research indicates high risk of UV-B induced eye and skin malignancies. The AIC and BIC of the regression models, indicates that the logarithm model provides the best fit for the relationship between UV-B absorbance and irradiance in the study locations considered. In other words, a change in the UV-B absorbance is proportional to the logarithm of the UV-B irradiance. Outdoor workers are therefore advised to take precautionary measures against over exposure to UV-B radiation in the study area.

REFERENCES

Estébanez, N., Gómez-Acebo, I., Palazuelos, C., Llorca, J., & Dierssen-Sotos, T. (2018). Vitamin D exposure and

risk of breast cancer: a meta-analysis. *Scientific reports*, *8*(1), 9039. https://doi.org/10.1038/s41598-018-27297-1

Grant, W. B. (2016). Roles of solar UVB and vitamin D in reducing cancer risk and increasing survival. *Anticancer research*, *36*(3), 1357-1370. https://doi: 10.1007/s11154-017-9415-2.

Hart, P. H., & Norval, M. (2018). Ultraviolet radiation-induced immunosuppression and its relevance for skin carcinogenesis. *Photochemical & photobiological sciences*, *17*(12), 1872-18. https://doi.org/10.1039/c7pp00312a

Hill, T. R., & Aspray, T. J. (2017). The role of vitamin D in maintaining bone health in older people. *Therapeutic advances in musculoskeletal disease*, *9*(4), 89-95. https://doi.org/10.1177%2F1759720X17692502

Holick, M. F. (2016). Biological effects of sunlight, ultraviolet radiation, visible light, infrared radiation and vitamin D for health. *Anticancer research*, *36*(3), 1345-1356.

International Commission on Non-Ionizing Radiation Protection. (2017). ICNIRP statement on diagnostic devices using non-ionizing radiation: Existing regulations and potential health risks. *Health physics*, *112*(3), 305-321. https://doi.org/10.1097%2FHP.0000000000000654

Karami, S., Colt, J. S., Stewart, P. A., Schwartz, K., Davis, F. G., Ruterbusch, J. J & Moore, L. E. (2016). A case–control study of occupational sunlight exposure and renal cancer risk. *International journal of cancer*, *138*(7), 1626-1633. https://doi.org/10.1002/ijc.29902

Katiyar, S. K., Pal, H. C., & Prasad, R. (2017). Dietary proanthocyanidins prevent ultraviolet radiation-induced non-melanoma skin cancer through enhanced repair of damaged DNA-dependent activation of immune sensitivity. In *Seminars in cancer biology* (Vol. 46, pp. 138-145). Academic Press. https://doi.org/10.1016/j.semcancer.2017.04.003

Kezic, S., & van der Molen, H. F. (2023). Occupational skin cancer: measurements of ultraviolet radiation exposure bring knowledge for prevention. *British Journal of Dermatology*, *188*(3), 315-316. https://doi.org/10.1093/bjd/ljac127

Löfgren (2017). Solar ultraviolet radiation cataract. *Experimental eye research*, *156*, 112-116. https://doi.org/10.1016/j.exer.2016.05.026

Lucas, R. M., Norval, M., Neale, R. E., Young, A. R., De Gruijl, F. R., Takizawa, Y., & Van der Leun, J. C. (2015). The consequences for human health of stratospheric ozone depletion in association with other environmental factors. *Photochemical & Photobiological Sciences*, *14*(1), 53-87. https://doi.org/10.1039/c4pp90033b

Mofidi, A., Tompa, E., Spencer, J., Kalcevich, C., Peters, C. E., Kim, J & Demers, P. A. (2018). The economic burden of occupational non-melanoma skin cancer due to solar radiation. *Journal of occupational and environmental hygiene*, *15*(6), 481-491. https://doi.org/10.1080/15459624.2018.1447118

Seckmeyer, G., Schrempf, M., Wieczorek, A., Riechelmann, S., Graw, K., Seckmeyer, S., & Zankl, M. (2013). A novel method to calculate solar UV exposure relevant to vitamin D production in humans. *Photochemistry and Photobiology*, *89*(4), 974-983. https://doi.org/10.1111/php.12074

Surdu, S., Fitzgerald, E. F., Bloom, M. S., Boscoe, F. P., Carpenter, D. O., Haase, R. F. & Fletcher, T. (2013). Occupational exposure to ultraviolet radiation and risk of nonmelanoma skin cancer in a multinational European study. *PloS one*, *8*(4), e62359. https://doi.org/10.1371/journal.pone.0062359

Sombo, T., Shivil, T. J., & Igbawua, T. (2021). Measurement and assessment of occupational exposure to solar ultraviolet radiation in Makurdi Metropolis, Benue State, Central Nigeria. *Radiation Science and Technology*, *7*(2), 32-40. https://doi.org/10.11648/j.rst.20210702.13

Tertsea, I., Barnabas, I., & Emmanuel, A. (2013). Average solar UV radiation dosimetry in Central Nigeria. *International Journal of Environmental Monitoring and Analysis*, *1*(6), 323-327 http://dx.doi.org/10.11648/j.ijema.20130106.18